Final Report:

High Harmonic Radiation Generation and Attosecond pulse generation from Intense Laser-Solid Interactions

Principal Investigator: *Prof. Alec Thomas*

Co-Investigator: *Prof. Karl Krushelnick*

Period of time report covered: *Aug 2012 - April 2016.*

Recipient Organization: *University of Michigan, 2074 Fleming Administration Bldg. Ann Arbor, Michigan 48109-1318, United States of America*

DOE award number: ER55145 / DE-SC0008352

Summary of findings

- First high harmonic generation in laser-solid interactions at 10^{21} Wcm^{-2}
- Demonstration of harmonic focusing
- Study of ion motion effects in high harmonic generation in laser-solid interactions
- Demonstration of harmonic amplification

Results and Findings

We have studied ion motion effects in high harmonic generation, including shifts to the harmonics which result in degradation of the attosecond pulse train, and how to mitigate them. We have examined the scaling with intensity of harmonic emission. We have also switched the geometry of the interaction to measure, for the first time, harmonics from a normal incidence interaction. This was performed by using a special parabolic reflector with an on axis hole and is to allow measurements of the attosecond pulses using standard techniques.

High order harmonic generation (HHG) from laser solid-density plasma interactions has been studied extensively [1–9, 12, 15]. It occurs when the surface electrons of the target are oscillated by an intense laser field to relativistic speeds, where strong nonlinear effects give rise to the re-radiation of harmonics of the fundamental laser frequency [3, 4, 6–9, 15]. While much analytical work has been performed by simplified oscillation mirror model [5, 10, 14], the understanding of HHG under realistic conditions is still very limited. Previous theoretical studies in HHG typically focused on the electron dynamics on interfaces [2, 5, 12] and the scaling of the harmonics to high intensities. Simulations typically are run with static ions for reasons of computational constraints. However, as the intensity increases, it is clear that the ponderomotive push of the laser pulse will eventually cause significant ion motion during the passage of the laser pulse. This motion will complicate the moving mirror by adding an additional time varying Doppler shift to the reflected electromagnetic radiation. This shift will cause a degradation of the attosecond pulse train formed from the harmonics.

The maximum number of harmonics that can be obtained from laser solid-density plasma interactions depends on many factors, such as the target plasma density, pulse length, shape, and intensity. Here, we use an incident Gaussian laser pulse of 20 fs (FWHM) and focus only on the effects of the plasma density on HHG. For a given laser intensity, higher plasma density implies higher restoring force for plasma oscillation, which limits the amplitude of the electron surface oscillations, therefore limiting HHG. In contrast, if the plasma density is too small, larger amplitude surface oscillations may become quickly unstable, resulting a distortion and broadening in HHG.

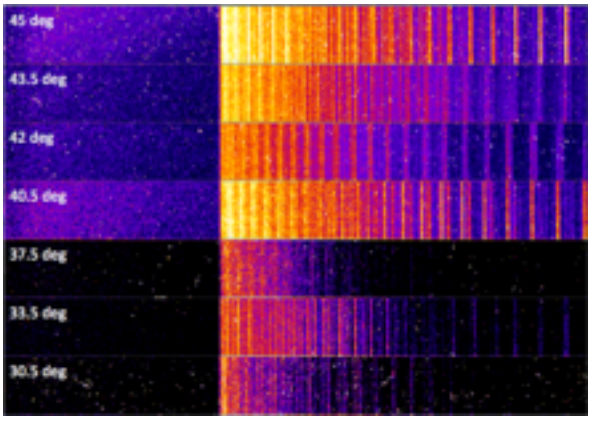

Fig 1: Raw harmonic spectra viewed from different angles with respect to normal. The cut off to the left is due to an aluminum filter. Longer wavelengths are to the right.

Experimental measurements were taken with the HERCULES laser to investigate the role of ion motion on HHG. Pulses from HERCULES were delivered to solid density targets with a 1 μm spot such that the on-target intensity was $2\text{x}10^{21}$ Wcm^{-2} (corresponding to $a_0 = 30$). Prior to the experimental chamber, mirrors focused the amplified pulse onto a pair of antireflection coated BK7 glass substrates acting as plasma mirrors. This contrast improvement prevented preplasma formation until ~1 ps before the main pulse interaction, maintaining a sharp density profile. With sufficiently high contrast, a well-defined reflection point exists at the relativistic critical density surface (i.e., when the plasma frequency equals the laser frequency). Varying the angle of incidence, the harmonic spectra show clear shifts. The spacing between harmonics changes, indicating that what is happening is a slight shift to the fundamental frequency. This is consistent with Doppler shifts of the laser pulse due to ion motion.

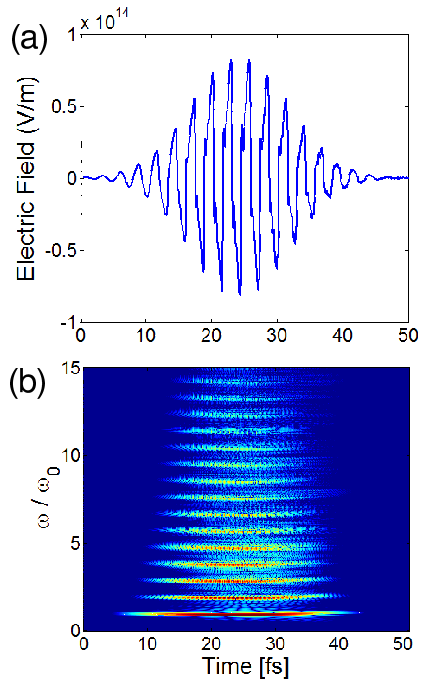

Fig 2: Gaussian pulse with intensity of 10^{21} Wcm^{-2} reflected off plasma with density $50n_c$. The reflected pulse (top) is shown with its Wigner transform (bottom)

To understand these results, simulations were performed by using a one-dimensional particle-in-cell (PIC) code, EPOCH [13]. The laser pulse is linearly polarized. The solid density plasma are made of electrons and Aluminum-27 ions. The effects of ion motion on the harmonic generation are thus investigated.

Figure 2 (a) shows an example of the reflected Gaussian pulse with intensity of 10^{21}W/cm^2 reflected off the plasma with density of $50n_c$, where n_c is the non-relativistic critical density of the plasma. Its Wigner transform is shown in Fig. 2 (b). The

number of harmonics up to 15 of the fundamental laser frequency ω_0 is clearly observed.

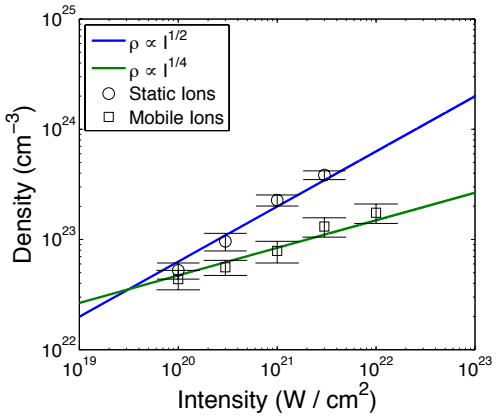

FIG. 3: Optimum densities for HHG as a function of pulse intensity from 1D PIC simulation, for both static ions and mobile Al-27 ions. Symbols represent the simulation data, error bars represent range of densities with equal number of observable harmonics, and solid lines represent curve fitting.

The optimum densities for maximum number of harmonic generation are shown in Fig. 3, for PIC simulations with both static ions and mobile Al-27 ions. It is found that the optimum density for HHG increases as the laser intensity increases, which scales as a with no ion motion but $a^{1/2}$ if ion motion is included. For the ultrarelativistic laser-plasma regime with no ion motion, the ultrarelativistic similarity theory [11, 14] states that the plasma-electron dynamics depends only on the similarity parameter $S = n_e/a_0 n_c = \text{const}$, where n_e is the plasma density, which implies that the optimum plasma density for HHG should scale as a_0, consistent with the observed scaling. However, with ion motion, the ion density compresses to a density proportional to $a^{1/2}$, which results in the observed scaling.

As seen from Fig.2 b, there is some degree of frequency shift in the harmonics within the duration of the reflected pulse, when mobile ions are used in the simulation. We confirm that this frequency shift is in fact the doppler shift of the pulse due to the net surface motion of the electron mirror. This net surface motion is caused by the non-negligible motion of the background ions during the process of laser plasma interaction. It is clear that the surface velocity follows closely the temporal envelopes of the incident laser pulse. The fundamental frequencies of the reflected pulse are obtained by looking at the peak values of the Wigner transform (the frequency of the largest magnitude for each moment in time). The frequency shifts also follow closely the envelope of the incident laser pulses. This may be easily understood as follows. When the laser intensity increases, the surface velocity increases, which would in turn introduce a larger frequency shift (i.e. larger Doppler red shift). Similarly, when the laser intensity decreases, the surface velocity will decrease, resulting a smaller frequency shift. We found that by adding a chirp to the laser pulse, these shifts can be compensated for, resulting in a cleaner attosecond pulse train once the fundamental has been removed.

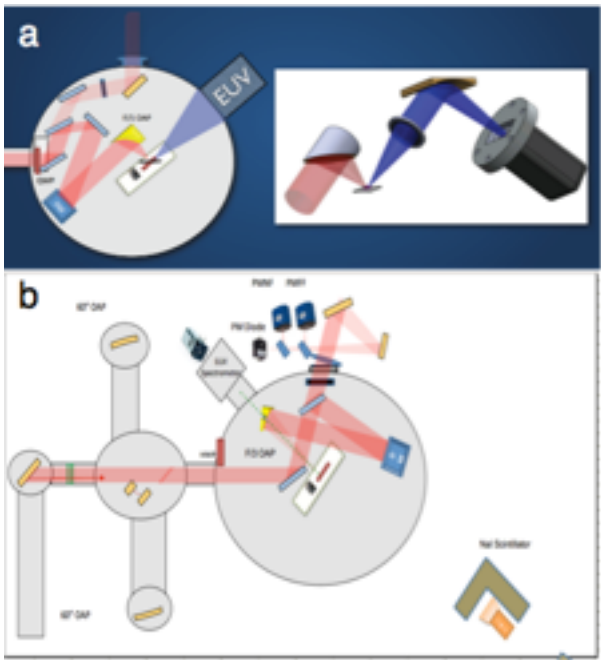

FIG. 4: Chamber set up. (a) configuration at 45 degrees incidence. (b) new configuration at normal incidence.

Another important piece of work for the project is switching the geometry to normal incidence. This is because for normal incidence, only the jxB force acts to generate harmonics instead of the E field directly. In this case, the oscillation is at 2ω, which means that only odd harmonics are generated. This is important because it will allow standard attosecond measurement techniques to be used, which rely on having only the odd harmonics.

To do this, a new chamber configuration was implemented as shown in figure 4. To allow measurement of the harmonics at normal incidence, a parabolic reflector with an on axis hole was developed. A student developed a technique to be able to drill a standard reflector but maintaining sufficient optical quality. The XUV spectrometer was then placed behind the parabola as in figure 4b so that the harmonics could be observed through the hole in the parabolic reflector.

A raw spectrum from the normal incidence interaction, compared with the 45 degree interaction, is shown in figure 5. This shows signatures of lines with larger intervals compared with the 45 degree incidence, consistent with the 2ω scaling.

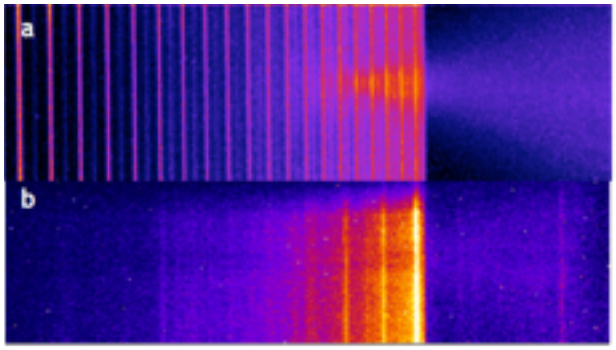

FIG. 5: Raw soft x-ray spectra generated by a laser incident on a target at (a) 45 degree incidence and (b) normal incidence. The cut off to the right is due to an aluminum filter. Longer wavelengths are to the left.

One crucial consideration for High-order Harmonic Generation (HHG) from solids is the density profile at the solid-vacuum interface. In particular, the preplasma formed by hydrodynamic expansion of the heated surface prior to the arrival of the main pulse. ***We have studied the effect of preplasma scale length on harmonic content using the HERCULES laser and through simulations. We found that there is an optimum scale length for harmonic production.*** This is significant for the development of the HHG source as we show that that the efficiency is very sensitive to the scale length.

Pulses from HERCULES were delivered to solid density targets with a 1 μm spot such that the on-target intensity was 2×10^{21} Wcm^{-2} (corresponding to $a_0 = 30$). Prior to the experimental chamber, mirrors focused the amplified pulse onto a pair of antireflection coated BK7 glass substrates acting as plasma mirrors. This contrast improvement prevented preplasma formation until ~1 ps before the main pulse interaction, maintaining a sharp density profile. With sufficiently high contrast, a well-defined reflection point exists at the relativistic critical density surface (i.e., when the plasma frequency equals the laser frequency).

To control the scale length of the preplasma, one or both plasma mirrors were replaced with a higher reflectivity optic. Control of the preplasma was also performed by using a secondary beam with a 63 ps delay and a variable intensity between 10^{12} and 10^{16} Wcm^{-2}. Optically polished fused silica and silicon wafer were used as the targets, with the substantial difference in damage threshold providing another means of controlling density. The experimental scalelength

was inferred from one-dimensional hydrodynamic simulations, which showed that it varied from 13 nm to 2.5 μm, corresponding to a range from a 60th to a 3rd of the laser wavelength.

An optimal scale length was determined to exist for strongly relativistic intensities. The optimum is due to a balance between requiring a longer scale length so that the plasma electrons can be effectively displaced allowing efficient movement of the critical density surface and requiring a short enough scale length as not to drive parametric instabilities. Although for longer scale lengths significant radiation is produced, the necessary coherence for attosecond pulse generation was lost.

Two-dimensional numerical simulations were carried out with the PIC code OSIRIS 2.0. Examining the plasma wave formation for longer scale lengths in 2D simulations, it can be seen that large amplitude surface plasma waves are generated and therefore strongly modulate the pulse resulting in a loss of coherence in the reflected wave. For short scale lengths the motion of the plasma is inhibited because the higher density plasma results in a higher restoring force ("stiffer spring") for the surface motion. These two competing processes lead to an optimum close to the plasma skin depth.

In addition, the special self-similarity of an exponential profile means that this optimum does not depend on intensity. Realistically, an upper limit in intensity invariance should exist, since the exponential density profile is truncated at some maximum density, which breaks the self-similarity. However, even for low atomic number solid density plasmas ($n > 100n_c$), this would require a temporally clean pulse with intensity $I >> 10^{22}$ W cm^{-2}. Hence, provided the target is not relativistically optically transparent, the only parameter that determines the optimal plasma dynamics for harmonic generation is the preplasma scale length.

(Published in Physical Review Letters: Scaling High-Order Harmonic Generation from Laser-Solid Interactions to Ultrahigh Intensity, F. Dollar, P. Cummings, V. Chvykov, L. Willingale, M. Vargas, V. Yanovsky, C. Zulick, A. Maksimchuk, A. G. R. Thomas, and K. Krushelnick PRL 110, 175002 (2013).

Another study we have performed is a computational investigation of harmonic generation from curved surfaces to generate collimated or focused coherent x-ray beams. With tight focusing, the harmonic beam generated is divergent, and conventional x-ray optics may be impractical for such conditions. Hence making use of curved surfaces may mitigate this effect. ***We have found that indeed focused harmonics can be produced with little loss in efficiency by interacting with curved surfaces.***

Using the OSIRIS 2.0 code, Gaussian, p-polarized laser pulses with field strength $a_0 = 35$ are focused to a beam-waist of 1 μm through the geometric focus of a spherically concave electron plasma target with density $100n_c$, with radial pre-plasma scale-length $L = \lambda/5$ and radius r.

The maximum field value achieved with the beam parameters here utilized is 4.7×10^{14}V/m. The highly oscillatory nature of the time-evolving maximal electric field magnitude is due to the

superposition of the incoming beam itself (which has a half-period of 8.4f s, roughly matching the temporal variation seen in Figure 2 as maxima would be expected to occur at twice the incoming frequency).

A geometry similar to the concave targets discussed in the previous section, but with parabolic profiles, were investigated in regard to their ability to collimate normal-incident laser pulses with the same parameters (see Figure 4). Although the investigation here summarized only focused on normal-incidence collimation, the same principles and variations would apply equally well to off-axis plasma parabolae.

The profile properties were chosen such that any ray passing through the point where the focus is defined would be collimated in the laser axis direction. A scale-length of $L = \lambda/5$ is assumed, the optimal in the experiments. A Fourier transform is taken of the p-component of the reflected electric field. The FWHM angular divergence of the beam is then calculated, and the harmonic content. The power law fall off of the harmonics varies slowly with L, while the collimation is significantly improved over the span of the simulation parameters, for similar laser intensities. This implies it may be feasible to focus the harmonics using structured targets in experiments *(publication in preparation).*

In the latter stages of the project, we hope to measure the attosecond pulse train. For normal incidence pulses, only odd harmonics are present. When the attosecond pulse strikes a krypton or argon gas target, atoms are photoionized and the electrons from the higher harmonics have kinetic energies on the order of 10 eV. One useful tool in photoelectron spectroscopy is the use of magnetic bottles in order to increase collection efficiency to as high a level as 50% for a 2π acceptance range.

Construction of the magnetic bottle began with design and initial construction of the solenoid to be used for the flight tube. The solenoid was to be placed inside a high-μ tube with diameter of around 2 inches. The program COMSOL Multiphysics was used to model the magnetic fields, including a solenoid and conical rare earth magnet, to construct the magnetic bottle. The next task is to track electrons through the fields.

High order harmonic generation (HHG) from laser solid-density plasma interactions is considered as a promising way to generate bright and ultrashort burst of x-rays. One of the key issues for HHG is the low conversion efficiency due to a power law fall off in harmonic intensity. Here, we explore a possible mechanism for HHG enhancement by reflecting an intense laser pulse mul- tiple times between two plasma surfaces. We find that HHG can be nonlinearly enhanced by orders of magnitude through multiple reflections compared with a single reflection. We argue this enhancement is due to the non-linear combination of the relativistically oscillating plasma mirror and the harmonic-rich pulse generated in preceding reflections. This mechanism should allow moderate power laser systems to efficiently generate coherent, ultrashort bursts of soft x-rays. High order harmonic generation (HHG) from laser solid- density plasma interactions has been studied extensively[1–14] due to its capability of generating phase-locked bursts of

harmonics into x-rays. The relativistic oscillating mirror mechanism[1,3,4] occurs when the surface electrons of the target are oscillated collectively by an intense laser field to relativis- tic speeds, such that a periodic Doppler shift due to the moving point of reflection gives rise to HHG of the laser frequency.

Previous theoretical studies in HHG typically focused on the electron dynamics on interfaces[1–4] and the scaling of the harmonics strength with drive laser intensity. The effect of the plasma density gradient was also recently studied.[10,12] However, the efficiency of HHG from a single laser surface interaction is still very low, especially with ultraclean surface conditions[12] or more moderate intensities. Thus, it is of interest to seek alternative configurations for efficient HHG.

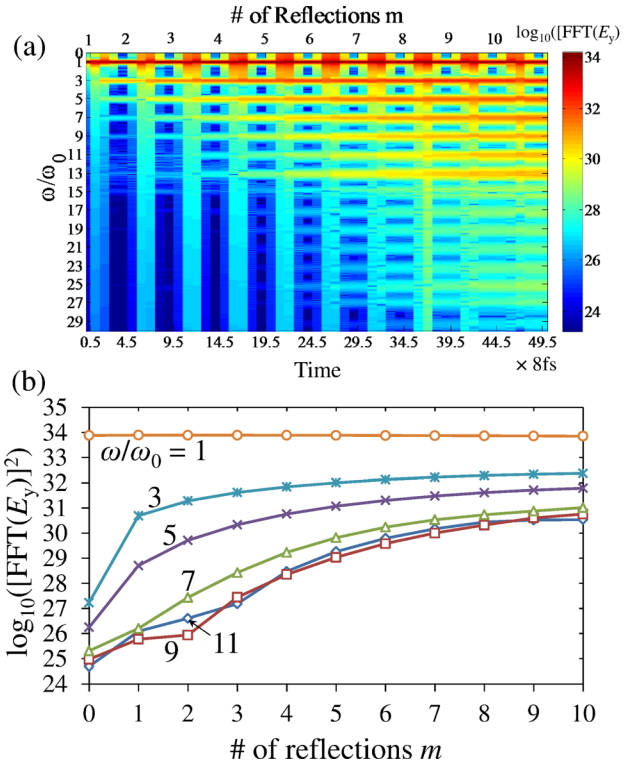

Fig 6 (a) The intensity spectrum of the laser pulse in Fig. 2, as a function of time (as well as number of reflections m) and frequency $x=x_0$. The ticks of the horizontal axes mark the beginning of each reflection. The lighter col- ored columns following the ticks approximately correspond to the duration of pulse reflection from one of the plasma surfaces. (b) The amplitude of the harmonic peaks as a function of m.

In this letter, we investigate the effect of multiple reflections of the laser pulse on HHG and show that the intensity of the high order harmonics can be nonlinearly enhanced, that is, increased beyond that from linearly adding the harmonics from each reflection. A schematic is shown in Fig. 1. This could be achieved in practice by propagating an intense laser pulse into a narrow capillary[15,16] at an angle of incidence ~1⁄4 p=4, for example. The rational is that by reflecting a laser pulse multiple times from two adjacent plasma surfaces, the harmonic components generated at one reflection may be enhanced at the subsequent reflections, providing a higher overall efficiency for HHG. By using particle-in-cell (PIC) simulations, we demonstrate that HHG can be enhanced by orders of magnitude from multiple reflections. We argue that this enhancement is due to the non-linear dynamics of plasma mirror motion, which is driven by the harmonic-rich pulse, as a result of the preceding reflections.

This is supported by comparing HHG from single reflection of a pristine pulse (of frequency x_0) with that of a pulse with one more harmonic component (of frequencies x_0 and nx_0, where $n > 1$ is an integer), based on both PIC simula- tions and simple analytical model. This mechanism, which enhances HHG by reflecting an intense pumping laser pulse superimposed on a weaker

harmonic pulse from a single solid plasma surface, may be considered as another effective method for HHG enhancement.

Recently, significant advances in peak power and rep- etition rate have been made in the technology of ultra- short pulse laser systems (pulse length < 100 fs) [1, 2]. These lasers enable the investigation of the "ultra- relativistic" regime in plasma physics, in which the laser electric field is far beyond that necessary to accelerate an electron to relativistic velocities (e.g., $I_0 \gg 10^{18}\mathrm{Wcm}^{-2}$). Laser-solid interactions at these intensities have many interesting applications including laser driven ion accel- eration, extreme ultraviolet and x-ray generation, and neutron generation [3–7].

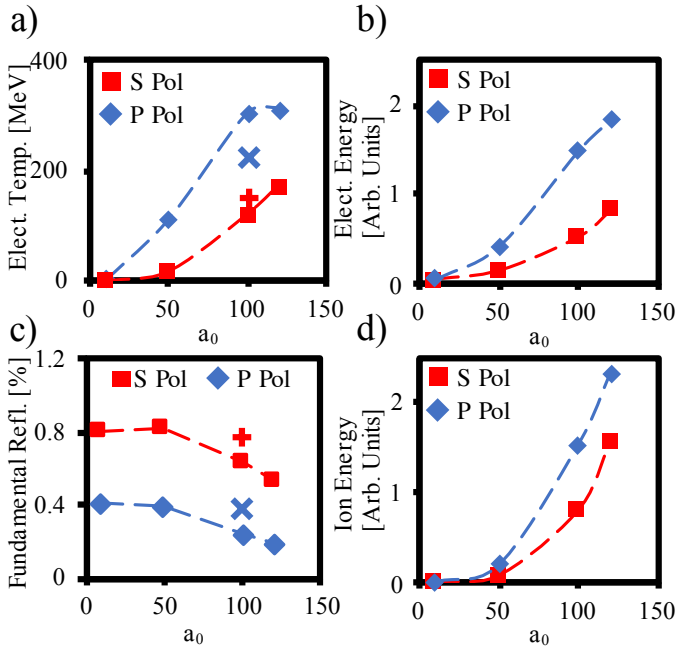

FIG. 4. (Color online) 3D PIC simulations for s (red squares) and p (blue diamonds) polarization. a) Electron temperature and c) reflectivity of the fundamental as a function of normalized vector potential. The case with fixed ions is shown with crosses. The energy absorbed into the particles as a function of intensity is shown for b) electrons and d) ions. Note that the lines are to guide the eye only.

A laser transfers energy efficiently to electrons in a plasma at the reflection point or "critical density", i.e., the point at where the laser frequency ω_0 is equal to the plasma frequency $\omega_p = 4\pi e^2 n_e/m_e$ (where e is the elec- tron charge, n_e is the electron density, and m_e is the mass of the electron). At electron densities below the critical density the plasma is transparent. At ultra-relativistic intensities, the laser imposes a substantial radiation pres- sure on the plasma and may displace the electrons and ions in the plasma, resulting in "hole-boring" [8]. The electrons respond much faster than the relatively mas- sive ions, so a thermal or electrostatic restoring force oc- curs if the electrons are displaced. However, during the laser pulse, energy can be transferred directly to the ions due to the electrostatic restoring force. For sufficiently thin plasmas, the radiation pressure may begin to accel- erate the ions uniformly, commonly known as the laser piston or radiation pressure acceleration (RPA) regime [9–11, 13].

Despite advances in laser technology, there is still sub- stantial difficulty in performing an experiment in this regime. Critically, the density profile of a solid density target when the

laser pulse arrives is rarely well char- acterized or controlled, causing substantial variations in the amount of laser energy absorbed and the number of hot electrons produced [12, 14, 15]. This preformed

plasma is generated from laser prepulses that are diffi- cult to avoid in modern laser systems. The amplified spontaneous emission (ASE) is a nanosecond duration pulse that causes hydrodynamic expansion of the target, resulting in an exponential preplasma density profile that typically extends many wavelengths into the vacuum [16]. For ultrathin targets, this can lower the density substan- tially, even to the point of being below critical density. The ratio of laser intensity between the main pulse and these prepulses is known as the “laser contrast” ratio. Since the laser focus is typically Gaussian-like, the pre- plasma profile is not spatially uniform across the focal diameter which can cause significantly higher laser ab- sorption [17, 18].

It is advantageous to develop scaling laws for laser ab- sorption based on laser intensity or fluence. However, in recent work distinct trends have begun to emerge that suggest that pulse duration is an important parameter that cannot be decoupled from intensity [19, 20]. One reason for this disparity is that the well established ab- sorption mechanisms such as Brunel or relativistic $\vec{J} \times \vec{B}$ absorption do not account for ion motion [21, 22]. In this Letter we isolate dominant absorption mechanisms at ultrahigh intensities by varying the incident polariza- tion and the target thickness. Conventional absorption mechanisms are present for thick targets and p polarized incident light, whereas they are suppressed for s polar- ization. For thin targets where the radiation pressure becomes significant a dramatic increase in absorption occurs. 3D particle-in-cell (PIC) simulations performed highlight the importance of ion motion in the absorption process, where deviations from 1D geometries cause the RPA to direct energy into thermal heating and electron and ion transverse momentum.

Published / in preparation

F. Dollar, P. Cummings, V. Chvykov, L. Willingale, M. Vargas, V. Yanovsky, C. Zulick, A. Maksimchuk, A. G. R. Thomas, and K. Krushelnick, Phys. Rev. Lett. 110, 175002 (2013)

E. C. Welch, P. Zhang, F. Dollar, Z. H. He, K. Krushelnick, and A. G. R. Thomas, Time dependent Doppler shifts in high-order harmonic generation in intense laser interactions with solid density plasma and frequency chirped pulses, Phys. Plasmas 22, 053104 (2015).

P. Zhang and A. G. R. Thomas, Enhancement of high-order harmonic generation in intense laser interactions with solid density plasma by multiple reflections and harmonic amplification, Applied Physics Letters 106, (2015)

F. Dollar, P. Cummings, V. Chvykov, L. Willingale, M. Vargas, V. Yanovsky, C. Zulick, A. Maksimchuk, A. G. R. Thomas, and K. Krushelnick, "Effect of ion motion on high harmonic generation in intense laser interactions with solid density targets" (in preparation)

F. Dollar, C. Zulick, V. Chvykov, L. Willingale, V. Yanovsky, A. Maksimchuk, A. G. R. Thomas, and K. Krushelnick "Trends in high intensity laser absorption at oblique incidence angles for solid density targets" (in preparation)

[1] G. D. Tsakiris, K. Eidmann, J. Meyer-ter-Vehn, & F. Krausz, New J. Phys., 8, 19 (2006) [2] S. Gordienko, A. Pukhov, O. Shorokhov,& T. Baeva, Phys. Rev. Lett., 93, 115002 (2004) [3] S. V. Bulanov, et al., Phys. Plasm. 1, 745 (1994).
[4] D. von der Linde and K. Rza`zewski, App. Phys. B 63, 499 (1996).

[5] R. Lichters, et al., Phys. Plasm. 3, 3425 (1996).
[6] P. A. Norreys, et al., Phys. Rev. Lett. 76, 1832 (1996).
[7] L. Plaja, L. Roso, K. Rza`zewski, and M. Lewenstein, J. Opt. Soc. Am. 7, 1904 (1998).
[8] N. M. Naumova, J. A. Nees, I. V. Sokolov, B. Hou, and G. A. Mourou, Phys. Rev. Lett. 92, 063902 (2004).
[9] H. Vincenti, S. Monchoce, S. Kahaly, G. Bonnaud, Ph. Martin and F. Quere, Nat. Communications 5, 3403 (2014).

[10] B. Dromey, et al., Nat. Phys. 8, 804 (2012).
[11] S. Gordienko, and A. Pukhov, Phys. Plasmas 12, 043109 (2005). [12] T. Baeva, et al., Phys. Rev. E 74, 046404 (2006).

[13] T. Arber, et al., EPOCH: Extendable PIC Open Collaboration. http://ccpforge.cse.rl.ac.uk/gf/project/epoch/, October 2011.

[14] T. Baeva, et al., Phys. Rev. E 74, 046404 (2006).

[15] F. Dollar, P. Cummings, V. Chvykov, L. Willingale, M. Vargas, V. Yanovsky, C. Zulick, A. Maksimchuk, A. G. R. Thomas, and K. Krushelnick, Phys. Rev. Lett. 110, 175002 (2013).